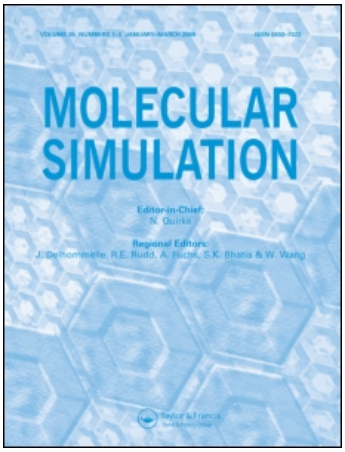

Molecular Simulation
Publication details, including instructions for authors and subscription information:
http://www.informaworld.com/smpp/title~content=t713644482

A Molecular Dynamics Study of the Vibrational Spectra of Silica Polyamorphs

Bertrand Guillot[a]; Yves Guissani[a]
[a] Laboratoire de Physique Théorique des Liquides, (CNRS URA 765) Université Pierre et Marie Curie, Paris Cedex 05, France

To cite this Article Guillot, Bertrand and Guissani, Yves(1997) 'A Molecular Dynamics Study of the Vibrational Spectra of Silica Polyamorphs', Molecular Simulation, 20: 1, 41 — 61
To link to this Article: DOI: 10.1080/08927029708024167
URL: http://dx.doi.org/10.1080/08927029708024167

Molecular Simulation, 1997, Vol. 20, pp. 41–61
Reprints available directly from the publisher
Photocopying permitted by license only

A MOLECULAR DYNAMICS STUDY OF THE VIBRATIONAL SPECTRA OF SILICA POLYAMORPHS

BERTRAND GUILLOT and YVES GUISSANI

Laboratoire de Physique Théorique des Liquides, (CNRS URA 765) Université Pierre et Marie Curie, Boîte 121, 4 Place Jussieu, 75252 Paris Cedex 05, France

(Received December 1996; Accepted January 1997)

The vibrational spectra (inelastic neutron scattering, infrared absorption and Raman scattering) of fused silica in the amorphous and in the liquid state are investigated by molecular dynamics simulation in using the TTAM interionic potential (Tsuneyuki *et al.*, *Phys. Rev. Lett.*, **61**, 869 (1988)). The simulation predicts in the low frequency region a boson peak, quite similar to the one observed experimentally in different spectroscopies. This mode is attributed to concerted motions between SiO_4 tetrahedra and involves the medium-range order in the glass. Upon densification the boson peak shifts to higher frequencies and is less pronounced. Correlatively, the evolution of the density of states with the temperature is found to be strongly dependent on the glass coordination, a finding which suggests an increasing fragility of silica glass with the pressure as recently proposed in the literature. Finally the inability of the TTAM potential to reproduce in details the density of states of silica glass is pointed out.

Keywords: Silica polyamorphs; vibrational spectra; TTAM potential

I. INTRODUCTION

For more than two decades a constant effort has been devoted to the elucidation of the molecular motions taking place in amorphous materials. Special attention has been paid to the picosecond and subpicosecond time scale in using Raman [1] and infrared [2] spectroscopy as well as neutron inelastic scattering experiment [3]. The low frequency region of these spectra is dominated by a strong feature, the boson peak, whose origin is rather controversial [4], while the high frequency region is characterized by

vibrational modes generally associated with local excitations of the basic units of the glass (e.g. the SiO_4 tetrahedra in silica glass). Since the work of Shuker and Gammon [5] it is usual to interpret the optical spectra of amorphous materials in terms of the vibrational density of states (VDOS) via light-to-phonons coupling coefficients which may exhibit strong variations with frequency [6]. Although the latter procedure is useful and leads to significant conclusions, it tends to somewhat obscure the nature of the dynamics under investigation. By contrast, in a computer experiment (e.g. a molecular dynamics simulation) as soon as the force field governing the system is determined it is easy, and *a priori* unambiguous, to evaluate any correlation function and power spectrum of interest simply from the computer generated trajectories of the molecules or atoms which make up the simulated sample. Curiously enough, since the remarkable work of Brawer [7] on the vibrational spectra of BeF_2 glass investigated by molecular dynamics (MD), very few simulation works have been dedicated to a complete and systematic analysis of the vibrational spectra associated with prototypical glasses (however see [8]). A noticeable exception is silica glass which has been the object of many simulation studies because of its importance in geosciences and in the glass industry. However, the information on the vibrational dynamics in fused silica which can be gleaned from this theoretical literature is generally limited to the evaluation of the VDOS at room temperature (e.g. in refs. [9–11]) but exceptionally to that of an optical spectrum (e.g. infrared spectrum in ref. [12]).

In the present study we have performed MD calculations to evaluate the mean square displacements of ionic species, the VDOS, the infrared and the Raman spectrum of a model of fused silica originally proposed by Tsuneyuki *et al.* [13] (TTAM) to describe the crystalline polymorphs of silica. A systematic comparison was done between experimental data (when available) and calculated quantities. Moreover we have investigated the influence of the temperature on the vibrational dynamics between room temperature and 4000 K, i.e. a range which covers at once the vitreous and the liquid state. Given the peculiar ability of silica to change coordination under pressure, from tetracoordinated at low and moderate pressure to hexacoordinated at very high pressure, we have also evaluated the effect of pressure on the vibrational dynamics. In this context it was attractive to examine if the conjecture recently proposed by Shao and Angell [14] namely, fused silica becomes fragile under pressure, had a counterpart in the short time domain probed by the vibrational spectra (see also the related work of Barrat *et al.* in this volume). Finally the present study sheds some light on the origin of the boson peak.

II. COMPUTATIONAL DETAILS

Among the interaction potentials currently used to model silica in computer simulations the TTAM model [13] is certainly one of the most accurate in spite of its simplicity. Originally designed to describe the crystalline phases of silica (with rather good results, although a refined version of this potential proposed by Van Beest *et al.* [15] gives some improvement for the structure, the elastic constants and the density of states of the polymorphs), its domain of applicability was extended to the liquid phase and to the vitreous state by Rustad *et al.* [16] and by Della Valle and Andersen [17]. A complete investigation of the liquid phase (liquid-vapour coexistence line, critical point and evolution of the liquid structure up to the megabar range) was next reported by us [18] in introducing a slight modification of the potential (called TTAMm) to avoid infrequent events, but catastrophic for the MD run, occuring above 4000 K with original model. The agreement with the known thermodynamic properties of fused silica is satisfactory for such an economical potential in computer time, but not excellent (e.g. the density of simulated silica at one bar is of the order of 2.5 g/cm^3 instead of 2.2 g/cm^3) and there is room for improvement (the related potential of Van Beest *et al.* [15] gives no improvement in the liquid state). At the present time no other potential is clearly superior to it and has been tested over so large a range of thermodynamic conditions (however see the discussion in Section IV).

Our simulated sample was composed of 256 SiO_2 units (768 particles) interacting via the TTAMm potential. In using periodic boundary conditions, the equations of motion of silicon and oxygen ions ($q_{Si} = +2.4e$ and $q_O = -1.2e$) were solved by the Verlet algorithm with a time step ranging from 1 fs at 4000 K to 4 fs at 300 K while an Ewald sum accounted for long range Coulombic interactions. The glassy states were generated from fully equilibrated configurations in the liquid phase, initiated between 4000 and 8000 K, and were progressively cooled by successive steps ($\Delta T = 500$ K) of quenching and equilibration of ~ 20 ps each. All the time correlation functions investigated here were averaged over different runs with independent initial conditions (e.g. at room temperature four or five runs of 80 ps each), a procedure needed by the slow convergence of the averaging in the glassy state (in the liquid phase the convergence is much faster). Finally notice that for strong glass formers like silica the dependence on the sample size (not investigated here) is not negligible (see [19]); neither is the role played by the huge cooling rate ($\sim 10^{12}$ K/s) currently used in computer simulations [20]. The combination of these latter two factors have two main

consequences: first the glass transition temperature of the model system is significantly overestimated, maybe by several hundred degrees for silica with the small systems ($\sim$ 1000 particles) and next, the glass obtained at low temperatures has not properly relaxed. So all comparison with real systems have to be done with these remarks in mind.

III. RESULTS

A. Mean Square Displacement

The movement of the silicon and oxygen ions within fused silica can be characterized by evaluating along the simulation run the time evolution of the mean square displacement (MSD) defined by

$$\langle \Delta r_i^2(t) \rangle = \langle (\vec{r}_i(t) - \vec{r}_i(0))^2 \rangle \tag{1}$$

where $\vec{r}_i(t)$ is the position of the particle of species i (Si or O) at time t and where the average is performed over all particles of the same species and all time origins. In Figure 1 are plotted on a log–log scale the MSD for silicon and oxygen ions from room temperature to 4000 K and for a silica density equal to 2.2 g/cm^3, 2.7 g/cm^3 and 4.0 g/cm^3, respectively, i.e. a range extending from cristobalite-like to stishovite-like density. Notice that the glass transition temperature in the present simulations is of the order of 2000 K and depends on the density ($T_g \sim$ 1800 K at 2.2 g/cm^3 and $\sim$ 2500 K at 4.0 g/cm^3). The time evolution of the MSD is characterized by three different regimes: (i) A kinetic regime at very short times ($t \lesssim 0.1$ ps) where $\langle \Delta r_i^2(t) \rangle \sim t^2$; (ii) A prediffusive regime extending up to the picosecond time scale where $\langle \Delta r_i^2(t) \rangle \sim t^n$ with $n < 1$, and (iii) A diffusive regime at long times ($t \gg 1$ ps) where $\langle \Delta r_i^2(t) \rangle \sim t$. In the kinetic regime, the amplitude of $\langle \Delta r_i^2(t) \rangle$ is proportional to the temperature and corresponds to harmonic motions. Thus in Figure 1 the MSD's are multiplied by 300 K/T(K) in order to evidence the linearity in temperature. The prediffusive (or caging) regime is reached when the time scale matches the time needed for the particle to explore the fluctuating cage where it is trapped. As seen in Figure 1, in the glassy state ($T < T_g$) this caging regime can last the entire length of the MD run, a prohibitive additional computer time being required to reach the diffusive regime. In fact for normal silica glass (2.2 g/cm^3 and 300 K) the time evolution of the MSD's is characterized by a strong overshoot near 0.2–0.3 ps followed by oscillations (in fact the oscillations are already visible

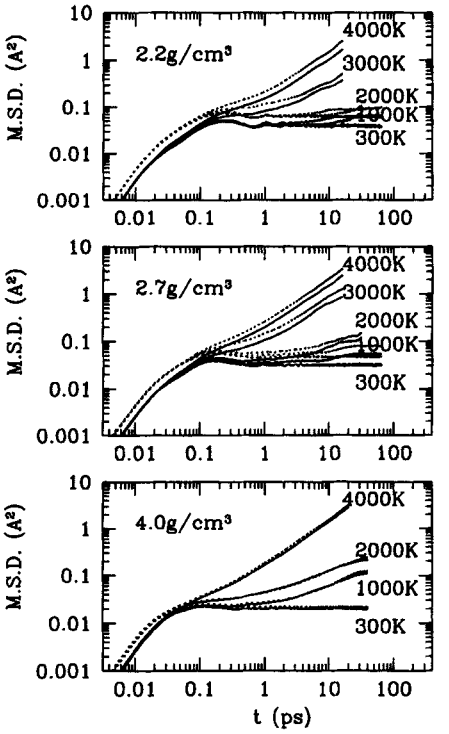

FIGURE 1 Mean square displacements of silicon (bold curves) and oxygen (dotted curves) ions in fused silica. For convenience the MSD's have been multiplied by 300 K/T(K) in order to emphasize the linearity with temperature at short times (see text).

in the preovershoot area), features which persist near T_g and disappear rapidly in the liquid state where diffusion occurs. In densified silica at 2.7 g/cm^3 the overshoot in the glassy state is much less pronounced and the oscillations are strongly damped. In the hexacoordinated glass at 4.0 g/cm^3 a quite different behaviour is observed since neither overshoot nor oscillations show up. Similar results have been obtained by Shao and Angell [14] with a less refined potential for silica. According to Angell's ideas the above findings suggest that in strong glasses (i.e. normal and moderately densified silica glass) anharmonicities of relatively large amplitude are tolerated by the system before diffusion occurs, while in more fragile glasses (e.g. ultra densified silica glass) the anharmonicities lead irreversibly to concerted motions and trigger the diffusion process. Furthermore this author stresses [21], without demonstrating it explicitly, that the peculiar oscillations exhibited by the MSD are due to the same motions which cause the famous

boson peak observed by Raman spectroscopy and inelastic neutron scattering [1, 22]. To investigate this point we have first evaluated the vibrational density of states, associated with our model glass.

B. Vibrational Density of States

A quantity directly connected to the above MSD's is the vibrational correlation function associated with species i (Si or O) namely

$$g_i(t) = \frac{1}{N_i} \sum_j \langle \vec{v}_j(t) \cdot \vec{v}_j(0) \rangle \tag{2}$$

where j runs over either the Si or the O ions. On the other hand, in an inelastic neutron scattering experiment, the generalized (or neutron weighted) density of states associated with a silica sample is given, in the incoherent approximation, by the following relationship [23]

$$g_N(\omega) = \sum_{i=\mathrm{Si,O}} \frac{\sigma_i c_i}{m_i} g_i(\omega) \tag{3}$$

where σ_i is the scattering cross section of species i, c_i the concentration, m_i the atomic mass and $g_i(\omega)$ the vibrational density of states associated with eq. (2), respectively, and where unimportant factors have been omitted. The important point is that the quantity $g_N(\omega)/\omega^2$ can be identified under specific conditions as the one-phonon scattering function as measured in neutron experiments [24]. The results of the MD calculations for $g_N(\omega)$ and $g_N(\omega)/\omega^2$ are collected in Figure 2. As far as the low frequency part of the $g_N(\omega)/\omega^2$ is concerned, the normal silica glass exhibits a pronounced peak in the boson peak region (~ 45 cm^{-1}) which lessens progressively with the temperature and is absent in the liquid phase at 4000 K. The agreement with the experimental data of Buchenau *et al.* [25] Malinovsky *et al.* [22] is impressive considering all sources of uncertainty (experimental and computational). In densified silica at 2.7 g/cm^3 (for which no experimental data are available) the same features are observed but the boson peak is shifted somewhat (~ 55 cm^{-1}), is less pronounced and decreases more rapidly with the temperature. As for the hexacoordinated glass at 4.0 g/cm^3, it displays a much weaker peak located around 80 cm^{-1} which vanishes near T_g(~ 2500 K). In summary, the simulation is both able to reproduce the observed boson peak in normal silica glass and to show that its attenuation under heating is consistent with the behaviour expected for a strong glass

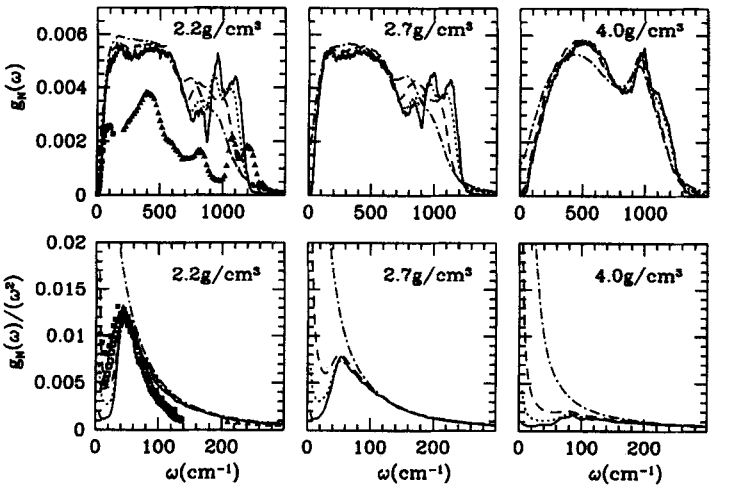

FIGURE 2 Evolution with the temperature and the density of the neutron weighted VDOS of fused silica. The curves correspond to the VDOS at $T = 300$ K (bold), 1000 K (dotted), 2000 K (dashed) and 4000 K (dashed dotted), respectively. The filled squares represent the inelastic neutron scattering data of Buchenau *et al.* [25] and the empty squares that of Malinovsky *et al.* [22] for normal silica glass at room temperature while the filled triangles are the corresponding high frequency data for Carpenter and Price [24]. The upper panels present plots of $g_N(\omega)$ in arbitrary units and the lower panels those of $g_N(\omega)/\omega^2$.

former [26]. Correspondingly, the disappearance of the boson peak at liquid temperature seems to be directly correlated to the damping of the oscillations in the MSD's, as suggested by Shao and Angell [14]. Furthermore, the fact that the simulation predicts a very different boson peak for silica glass at stishovite density supports the conclusion that highly compressed silica is much more fragile than the normal glass (according to the observation that a glass is all the more fragile when the boson peak is weak [26]). Finally upon further consideration it appears that the shift of the boson peak with density in the frequency domain can be correlated with the onset of the caging regime exhibited by the MSD's (observe in Fig. 1 how much earlier the caging regime starts when the density increases).

At higher frequency ($\omega > 100$ cm^{-1}) the comparison (see Fig. 2) with inelastic neutron scattering data of Carpenter and Price [24] shows that the calculated VDOS reproduces semi-quantitatively the former ones. More precisely the experimental high frequency band ($\sim 1100-1200$ cm^{-1}) is predicted at a lower frequency ($\Delta\omega \sim 100$ cm^{-1}) and the band near 400 cm^{-1} is not sufficiently intense in the calculated profile. On the other hand the intermediate band near 800 cm^{-1}, as well as the LO-TO splitting of the

high frequency band (according to the terminology used in the literature [27]), are well reproduced (the assignment of these bands will be detailed below). But a new remarkable feature is apparent in the evolution of the VDOS with the temperature (no experimental data are available except the fragmentary work of ref. [28]). Instead of an expected global low frequency shift of the position of the modes when the temperature increases, there is a pronounced evolution of the high frequency modes (e.g. 800, 1000 and 1100 cm^{-1}) in going from the glassy state to the liquid state (for example see in Fig. 2 how the 800 and 1000 cm^{-1} modes merge at 2000 K). The same type of behaviour is observed in densified silica at 2.7 g/cm^3 while in ultradense silica at 4.0 g/cm^3 a quite different situation occurs. Indeed, the VDOS evolves very little in the glassy state (300–2000 K) and more markedly above T_g ($\sim$ 2500 K), the low frequency part of the density of states being then the most affected one. Notice also the significant redistribution of the vibration modes in going from tetracoordinated silica to hexacoordinated silica. This redistribution was already pointed out by Rustad *et al.* [16] with the TTAM potential and by Jin *et al.* [29] with a more sophisticated three-body potential. Thus the classification between strong and fragile glasses seems still relevant for silica on the ultrashort time scale (10^{-13}s–10^{-15}s) considering that at low and moderate pressure, silica shows a progressive evolution of its high frequency excitations with temperature even in the glass transition region (as expected for a strong glass), while in ultradense silica the dynamics varies abruptly when T approaches T_g, the very definition of fragile behaviour.

In order to better understand the genesis of the boson peak and the high frequency modes in normal silica glass, we have evaluated by MD the density of states of oxygen and silica ions associated first with an isolated $SiO_4^{-2.4e}$ unit interacting via the TTAM potential and next when this unit is immersed in the force field generated by a frozen silica matrix. In the latter case the density of states was averaged over 256 different configurations of the frozen matrix. The density of states of our isolated $SiO_4^{-2.4e}$ unit (stick spectrum in Fig. 3) displays four main bands, as expected for T_d symmetry [30], located at 337, 504, 768 and 793 cm^{-1}, respectively plus a number of much weaker combination bands due to mode coupling (notice that the full Hamiltonian of the SiO_4 unit is used in the MD calculation). Interestingly enough, the bands at 337 cm^{-1} and 793 cm^{-1} only involve the oxygen ions and are associated respectively with E symmetry (bending and twisting) and A_1 symmetry (symmetric stretching). As for the intermediate bands at 504 and 768 cm^{-1} they involve at once the motions of silicons and oxygens and are due to deformation modes of F_2 symmetry (asymmetric stretching and bending).

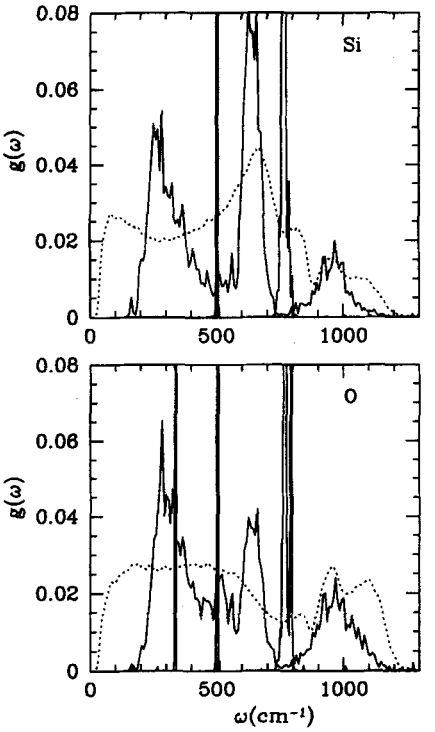

FIGURE 3 The VDOS for an isolated $SiO_4^{-2.4e}$ tetrahedron (stick spectrum), a SiO_4 unit immersed in a frozen silica matrix (bold curves) and a silica glass at room temperature (dotted curves). The upper panel shows the motions of the silicons and the lower panel those of the oxygens. Notice also that the four fundamentals of an isolated $SiO_4^{-2.4e}$ are located at $\nu_1(A_1) = 793\,cm^{-1}$, $\nu_2(E) = 337\,cm^{-1}$, $\nu_3(F_2) = 504\,cm^{-1}$ and $\nu_4(F_2) = 768\,cm^{-1}$, respectively.

The effect of the frozen matrix on these vibrational bands is considerable since the resulting density of states now exhibits three broad bands (the curves shown in Fig. 3 correspond to a SiO_4 unit thermally equilibrated at 300 K) very vaguely reminiscent of the vibrational modes of an isolated SiO_4. Consequently it is difficult to give a clear attribution to these bands. However, in using symmetry adapted coordinates one can show, for example, that Si—O stretching is mainly responsible for the high frequency band near 1000 cm^{-1} and partly contributes to the intermediate band around 650 cm^{-1} while it contributes negligibly to the low frequency band. One notices also that the densities of states of the oxygen and silicon ions are now very similar to each other. In comparing the latter ones with that obtained in the silica glass, two features are striking. First the reshaping of the density of states in going from the frozen matrix to the thermally

activated glass is very significant since the distribution of modes between the oxygens and the silicons becomes highly asymmetrical especially in the low and intermediate frequency region (100–700 cm^{-1}). Next, and most importantly, the boson peak appears only with the glass: it is absent from the density of states of a SiO_4 unit immersed in a frozen silica matrix. In fact in the latter case there is no contribution below 120 cm^{-1}. So the boson peak is the result of a collective excitation involving the concerted motions of several SiO_4 units in the glass.

C. Infrared Absorption

In infrared spectroscopy the absorption coefficient $\alpha(\omega)$ is related to the Fourier transform, $I(\omega)$, of the autocorrelation function of the total dipole moment by,

$$\alpha(\omega) = \omega(1 - e^{-\hbar\omega/k_B T})\, I(\omega) \tag{4}$$

where unimportant factors have been omitted. In the framework of the TTAM model where silicons and oxygens possess a screened charge and are non polarizable, $I(\omega)$ can be expressed in terms of the Fourier transform, $g_J(\omega)$, of the autocorrelation function of the total charge current $\vec{J}(t) = \sum_i q_i \vec{v}_i(t)$, namely

$$I(\omega) = g_J(\omega)/\omega^2 \tag{5}$$

However, for frequencies higher than $k_B T$ (~ 200 cm^{-1} at 300 K) a classical profile as the one obtained for $g_J(\omega)$ by MD calculation, has to be corrected for quantum effects and especially for the principle of detailed balance (i.e. $g(-\omega) = e^{-\hbar\omega/k_B T} g(\omega)$). Although a really accurate quantum correction to desymmetrize a classical spectrum for $\omega > k_B T/\hbar$ is still an open question, some approximate procedures do exist (see ref [31]). One of these is particularly convenient,

$$g_J(\omega) = \frac{\hbar\omega}{k_B T} \frac{1}{(1 - e^{-\hbar\omega/k_B T})} g_J^{cl}(\omega) \tag{6}$$

where $g_J^{cl}(\omega)$ is the profile calculated by MD. Hence, the absorption coefficient (4) is, very simply,

$$\alpha(\omega) \equiv g_J^{cl}(\omega) \tag{7}$$

The calculated absorption spectrum for normal silica glass at room temperature is compared in Figure 4 with the experimental data of Velde and Couty [32a,b] beyond 400 cm^{-1} and with compilation data of Strom and Taylor [2] below 400 cm^{-1}. Here again the agreement is only semi-quantitative. Although the three main bands (located experimentally about 470, 800 and 1100 cm^{-1}, respectively) are clearly present in the calculated spectrum, the position of the two strongest bands is not accurately reproduced (~ 600 cm^{-1} instead of 470 cm^{-1} and ~ 950 cm^{-1} instead of 1100 cm^{-1}) neither is their relative intensity, while the intermediate band is buried under the tails of the side bands. Part of the above discrepancies could be due to insufficient quantum corrections and to the neglect of induced dipoles. In comparing the VDOS, $g_N(\omega)$, shown in Figure 2 with the infrared absorption one notices that some vibrational modes are cancelled

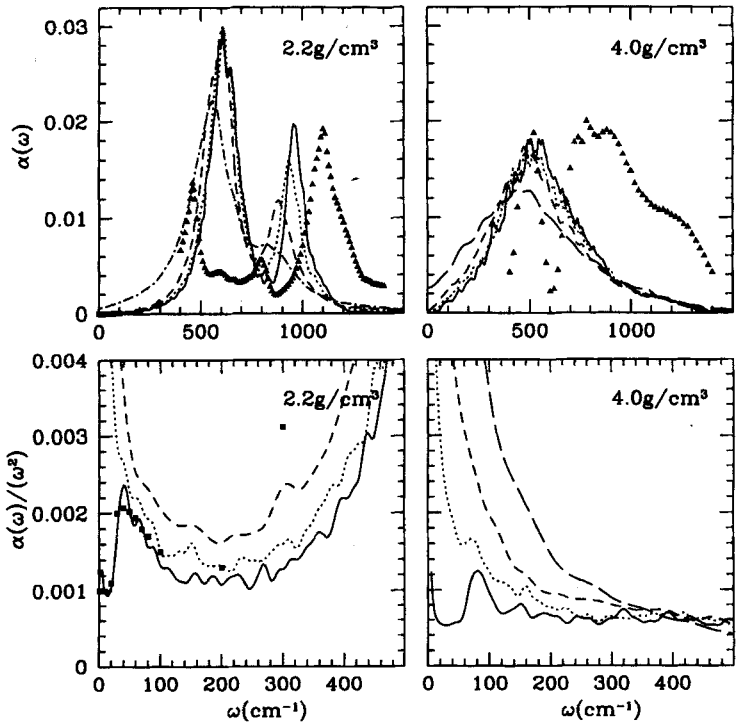

FIGURE 4 The far infrared spectrum of fused silica between room temperature and 4000 K (same symbols as in Fig. 2) at normal (2.2 g/cm^3) and very high (4.0 g/cm^3) density. The filled squares correspond to the data of refs. [12] and [33] while the filled triangles are the data of Velde and Couty [32b]. The upper panel is a plot of the absorption coefficient in arbitrary units and the lower panel that of the intensity $\alpha(\omega)/\omega^2$.

while others are enhanced by virtue of the selection rules imposed by the definition of the collective variable $\vec{J}$. For example, most of the intensity of the low frequency band of the VDOS is infrared inactive and the interaction induced splitting of the high frequency band is reduced to a weakly dissymetric band in the infrared spectrum. Nevertheless, the simulation also predicts a clear signature of the boson peak (see Fig. 4) in the 50 cm^{-1} region. This peak was actually observed by Wong and Whalley [33] and Stolen *et al.* [34] as reviewed by Strom and Taylor [2] and was related at that time, to an ill-defined shoulder on the low frequency flank of the inelastic neutron scattering spectrum. The present simulation results corroborate this view and confirm that the same mechanism is at the origin of the boson peak observed in both spectroscopies (neutron and infrared).

The effect of the temperature on the absorption spectrum is to shift the envelope of the calculated profile to lower frequencies and to decrease the intensity of the bands, especially the high frequency band, the evolution being progressive between room temperature and 4000 K (see Fig. 4). These trends are fully supported by the experimental data of Neuroth [35], Markin and Sobolev [36] and Gaskell [37] on fused silica between room temperature and approximately 2000°C (molten quartz). Notice also that the simulation predicts the absence of the boson peak above 1000 K.

Under moderate pressure (up to tens of kilobars) the experimental infrared spectrum of silica glass changes very little [32b] apart from the appearance of sub structure bands in the intermediate region (600–800 cm^{-1}), a slight broadening of the high frequency band and a shallow splitting of the low frequency band. The same features are obtained by MD in increasing the density from 2.2 to 2.5 and even 2.7 g/cm^3 (not shown). On the other hand, the change of coordination from fourfold to sixfold induced by very high pressures (hundreds of kbar) is striking in the absorption spectrum. Williams *et al.* [38a,b] in measuring infrared spectra of silica (polymorphs and glass) to pressures of 400 kbar have pointed out a strong decrease of the high frequency band at these pressures and an enhancement of the relative amplitude of the intermediate band (700–900 cm^{-1}). These spectral features were attributed to the decrease of the number of SiO_4 tetrahedra concomitant with a rapid increase of SiO_6 octahedra with the pressure. The agreement with our calculation for silica glass at 4.0 g/cm^3 shown in Figure 4 is patent even if in the details the simulated spectrum does not coincide accurately with the experimental one. In fact only one broad band peaking around 500 cm^{-1} is obtained by simulation, this broad band arising from the low frequency shift of the high frequency band which then merges into the low frequency band. Finally, the

calculated absorption spectrum shows a weak temperature dependence in the glassy state and a more significant one in the liquid state (see also the behaviour of the VDOS in previous section).

D. Raman Scattering

Even in the framework of the simple TTAM model for silica, the Raman spectrum cannot be evaluated as easily as the infrared one because supplementary information about polarizability distorsions induced by the interactions in the melt is required. A suitable model of the interaction-induced contributions to the ionic polarizability has been developed by Madden *et al.* [39a,b] for alkali halide melts and can be readily extended to fused silica. Thus, the instantaneous polarization of a system composed of N ions and subjected to an external electric field $\vec{E}_0$ is the sum of individual induced dipoles.

$$\vec{\mu}_i = \overleftrightarrow{\alpha}(R^N)\left\{\vec{E}^0(\vec{r}_i) + \sum_j \overleftrightarrow{T}(\vec{r}_{ij})\vec{\mu}_j\right\} \tag{8}$$

where $\vec{\mu}_i$ and $\vec{r}_i$ are the induced dipole and position of ion i, respectively, $\overleftrightarrow{T}$ is the dipole-dipole tensor and $\overleftrightarrow{\alpha}_i(R^N)$ is the instantaneous polarizability tensor of ion i which depends, a priori, on the relative position of all other ions of the sample. Notice that equation (8) is quite general and has been widely used to investigate the light scattering spectrum in molecular solids, liquids and gases [40] where the dipole-induced dipole DID mechanism plays the leading role (in that case $\overleftrightarrow{\alpha}_i$ is simply the gas phase polarizability tensor of the molecule i).

In ionic materials the strong Coulombic interactions render the ionic polarizability $\overleftrightarrow{\alpha}_i(R^N)$ strongly dependent on the environment. As emphasized by Fowler and Madden [41], two main effects may contribute to modulate the intrinsic polarizability of an ion: (i) The electric distortions induced by the ionic field at the site of the ion and (ii) The short range overlap interactions between the ion and its immediate neighbours. Assuming that these two mechanisms are additive, the instantaneous polarizability of an ion is,

$$\overleftrightarrow{\alpha}_i(R^N) = \bar{\alpha}_i\overleftrightarrow{I} + \overleftrightarrow{\Delta}\alpha_i^C(R^N) + \overleftrightarrow{\Delta}\alpha_i^{SR}(R^N) \tag{9}$$

where $\bar{\alpha}_i$ is the mean polarizability (in an isotropic environment) of the ion, $\overleftrightarrow{\Delta}\alpha_i^C(R^N)$ is the change in the polarizability due to the ionic field and field

gradient and $\vec{\Delta}\alpha_i^{SR}(R^N)$ is the contribution due to short range overlap disortions. At this stage it is possible to evaluate by MD simulation the total polarization of the system by iterating, at each MD step, the equation (8) where the expression (9) of the ionic polarizability has been first introduced. Although this type of calculation has been performed successfully by Madden *et al.* [39a] for alkali halide melts, it requires the knowledge of ionic hyperpolarizabilities (to evaluate $\vec{\alpha}_i^C$) and the explicit functional form of the short range overlap contribution: none of which are easily at hand in the case of silica. Furthermore the full calculation involves many summations and coupled terms which makes the interpretation of the results difficult. For these reasons we prefer, in a first attempt, to propose a simplified approach based upon realistic assumptions. In this approach the basic units of the system (silica glass) are the SiO_4 tetrahedra. Next the iteration procedure in eq. (8) is truncated at the first order so that the macroscopic polarization taken by the sample may be written as

$$\vec{P} = \sum_i \left\{ \vec{\alpha}_i(R^N) + \bar{\alpha}^2 \sum_j \vec{T}_{ij}(\vec{r}_{ij}) \right\} \vec{E}_0 \tag{10}$$

where $\vec{\alpha}_i$ is the fluctuating polarizability tensor of the SiO_4 unit i, $\bar{\alpha}$ is the mean polarizability of the SiO_4 unit, $\vec{T}$ the dipole–dipole tensor and $\vec{r}_{ij}$ is the distance between two SiO_4 units (approximated by the Si–Si distance). The polarizability of silicon ion being negligible as compared with that of oxygen ion ($\bar{\alpha}_O \sim 3.9$ A^3 and $\overline{\alpha_{Si}} \sim 0.17$ A^3) the mean polarizability of a SiO_4 unit is approximated by $4\bar{\alpha}_O$. Notice that in eq. (10) the DID mechanism is effective only between SiO_4 units considered as a whole while the DID contribution arising from the interactions within the tetrahedral units is neglected. In fact we know that the DID mechanism is expected to be almost cancelled when the system possesses a high local symmetry like an inversion symmetry (e.g. atomic liquids) or a T_d symmetry in the case of SiO_4. By analogy with eq.(9) the fluctuating polarizability of a SiO_4 unit i is due to a field gradient and field contribution, $\Delta\vec{\alpha}_i^C$, plus a short range overlap term $\Delta\vec{\alpha}_i^{SR}$. Although the functional form of the latter term is not exactly known, it is related to the repulsive part (hard core like) of the interionic potential for silica and can be considered as pairwise additive. Thus a convenient choice would be to assume that

$$\Delta\vec{\alpha}_{SiO_4}^{SR} = \sum_{i \neq j} A_{ij} \, e^{-(r_{ij} - \sigma_{ij})/b_{ij}} \vec{I} \tag{11}$$

where the indices i and j run over the silicon and the oxygens of the SiO_4 unit and σ_{ij} and b_{ij} are parameters which can be in principle deduced from the Si—O and O—O repulsive terms of the TTAM model [13]. Notice also that the above polarizability tensor is assumed isotropic, a reasonable choice for nearly perfect tetrahedral units. Finally according to the results of Madden *et al.* [39a] we neglect the hyperpolarizability contributions with respect to the short range ones (i.e. $\Delta\alpha^C \ll \Delta\alpha^{SR}$).

With this simplified model, the Raman intensity is given by

$$I(\omega) \equiv \int_{-\infty}^{\infty} dt\, e^{-i\omega t} \left\langle \left(\vec{k}_I \cdot \left\{ \sum_i \Delta\alpha_i^{SR}(0)\, \vec{\vec{I}} + \bar{\alpha}^2 \sum_{i,j} \vec{\vec{T}}_{ij}(0) \right\} \vec{k}_S \right) \right.$$
$$\left. \times \left(\vec{k}_I \cdot \left\{ \sum_i \Delta\alpha_i^{SR}(t)\, \vec{\vec{I}} + \bar{\alpha}^2 \sum_{i,j} \vec{\vec{T}}_{ij}(t) \right\} \vec{k}_S \right) \right\rangle \tag{12}$$

where $\vec{k}_I$ and $\vec{k}_S$ are the wave vector of the incident and scattered light, respectively, and where unimportant factors have been omitted. From the above expression it is obvious that the VV spectrum results from the short range overlap contribution to the polarizability while the VH spectrum arises exclusively from the DID mechanism between SiO_4 units. For computational convenience, in evaluating the polarized spectrum (VV), it is preferable to use the relative velocities within the SiO_4 units instead of the relative distances as indicated by eq. (11). Indeed, in the glassy state the harmonic approximation is valid for $T \ll T_g$ (see the discussion in Section A) and consequently the evaluation of a time correlation function associated with a quantity depending on the relative distances within a SiO_4 unit can be substituted by that of the corresponding relative velocities (see [7]). In the present case the polarized spectrum was evaluated from the autocorrelation function of the group breathing velocities [8],

$$C(t) = \left\langle \sum_i V_{(SiO_4)i}(t) \sum_i V_{(SiO_4)i}(0) \right\rangle,$$

where

$$V_{SiO_4}(t) = \sum_{i \neq j} (\vec{v}_i(t) - \vec{v}_j(t)) \cdot \frac{\vec{r}_{ij}(t)}{|r_{ij}|} \tag{13}$$

the indices i, j running over the silicon and the oxygens of the corresponding SiO_4 unit. Notice that in using the above procedure we have neglected the different weighting between Si—O and O—O interactions which appears in

eq. (11): this is immaterial for our purpose. As for the depolarized spectrum it is evaluated directly from its present definition,

$$I^{VH}(\omega) \equiv (4\bar{\alpha}_O)^4 \int_{-\infty}^{\infty} dt\, e^{-i\omega t} \left\langle \sum_{i \neq j} T_{ij}^{\alpha\beta}(t) \sum_{i \neq j} T_{ij}^{\alpha\beta}(0) \right\rangle \tag{14}$$

where

$$T_{ij}^{\alpha\beta} = \frac{1}{r_{ij}^3} \left(\frac{3 r_{ij}^{\alpha} r_{ij}^{\beta}}{r_{ij}^2} - \delta_{\alpha\beta} \right) \tag{15}$$

the indices i, j running over the silicon ions of the simulated sample. A qualitative and important difference distinguishes the VH spectrum from the VV spectrum. The former probes specifically the medium-range order typical of glassy systems [42] (notice the $1/r^3$ weighting factor in the definition (15)) , while the VV spectrum describes more local fluctuations (those of SiO_4 units) which depend only implicitly, through the interactions, on the medium-range order.

In practice the evaluation by MD of the polarized Raman intensity of normal silica glass gives a reduced spectrum, $\omega I^{VV}(\omega)/(n(\omega)+1)$ (where $n(\omega)+1 = (1-e^{-\hbar\omega/k_B T})^{-1}$ is the Bose factor), quite similar to the VDOS (compare Fig. 5 with Fig. 2). On the other hand the depolarized spectrum is significantly different since the intermediate frequency region ($500-900\,cm^{-1}$) is magnified at the expense of the other spectral regions : a feature corroborated by the experimental data [43]. However the computed spectra do not reproduce quantitatively the observed ones (see Fig. 5). In particular the main band peaking around $490\,cm^{-1}$ in the experimental polarized Raman spectrum is badly reproduced but this is not too surprising considering at once the disagreement reported for the VDOS (see Fig. 2) in this frequency region and to some extent the approximations made in the present calculation. Nevertheless, the boson peak around $50\,cm^{-1}$ is clearly present in the simulated spectra and matches quite well the data, especially the VH spectrum of Malinovsky *et al.* [22] (the boson peak is better viewed in the corrected representation $I(\omega)/\omega(n(\omega)+1)$ presented in Fig. 5). The latter point is particularly important since the calculated depolarized intensity is sensitive to the collective excitations revealed by Si—Si motions. Upon heating, the high frequency region above $600\,cm^{-1}$ of the simulated intensities shifts to lower frequencies and decreases in amplitude so that the presence of high frequency peaks around $1000\,cm^{-1}$ becomes barely visible

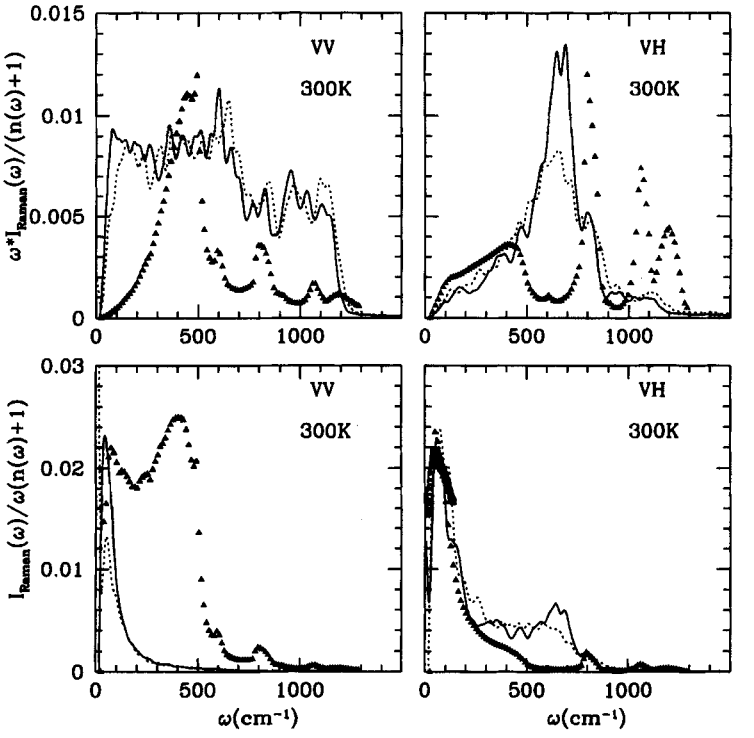

FIGURE 5 The Raman spectrum of normal silica glass at 2.2 g/cm^3 (continuous curves) and densified glass at 2.7 g/cm^3 (dotted curves). The upper panels show the reduced Raman intensity and the lower panels display the temperature corrected Raman intensity (notice that the ratio of the former one to the latter one is proportional to ω^2). The filled squares are the experimental data of McMillan *et al.* [43] and the empty squares correspond to the experimental VH spectrum of Malinowsky *et al.* [22] for normal silica glass.

as soon as T_g is reached (not shown): a finding also supported by the recent high temperature investigation of Mc Millan *et al.* [44]. Upon densification (e.g. 2.7 g/cm^3 in Fig. 5) the simulated glass presents a slight narrowing and high frequency shift of the low frequency band in the polarized spectrum while the depolarized spectrum exhibits a decrease of the 600–1200 cm^{-1} region. These results are in a qualitative agreement with experimental investigations [43]. Finally, the effect of the densification on the boson peak is weak while the effect of the temperature (not shown) is quite similar to that observed for the VDOS. Notice that all the above results only concern the tetracoordinated glass in which SiO_4 units can be identified unambiguously.

IV. CONCLUSION AND DISCUSSION

In this study we have shown by MD calculation that the use of the TTAM interionic potential for silica permits us to reproduce the main features of the vibrational spectra of silica glass. In particular the simulation predicts in the low frequency region a boson peak quite similar to the one observed experimentally in different spectroscopies. This mode is attributed to concerted motions between SiO_4 tetrahedra and involves the medium-range order in the glass. Moreover we have also shown that upon densification the boson peak shifts to higher frequencies and is less pronounced, whereas at very high pressures the gradual transformation of the tetracoordinated glass into an hexacoordinated glass results in a redistribution of the low and high frequency modes of the density of states. Correlated with this redistribution of modes, the evolution of the density of states with the temperature is found to be strongly dependent on the glass coordination, a finding which indicates an increasing fragility of silica glass with the pressure, as recently suggested in the literature [14, 15].

In spite of the above success, the simulation fails to reproduce accurately the experimental spectra, especially in the 200–600 cm^{-1} region where a pronounced peak is observed and in not properly accounted for by the calculation. In the same way the Si—O stretching band near 1100–1200 cm^{-1} is predicted at a lower frequency (by roughly 10%), a disagreement which was already encountered in lattice dynamics calculations [46, 47] of α-quartz and α-cristobalite interacting via the TTAM model. All these departures are attributed to inaccuracies in the interaction potential (the price to pay for its simplicity). A survey of the literature to trace clues for improvement is rather instructive. For example the BKS potential [15, 48], which is closely related to the TTAM potential, except that the repulsion-dispersion parameters were tuned to reproduce at best the structure and elastic constant of α-quartz, gives little improvement for the lattice dynamics but results in a better description of the Si—O stretching mode. More generally, the ionic pair potentials available in the literature are unable to reproduce with a great accuracy the VDOS even if some localized improvement can be reached [9] by an ad hoc adjustment of the parameters (but then the structure can deteriorate). Paradoxically enough, the introduction of three-body terms, with the objective to enhance the propensity for tetracoordination is not, frankly, rewarding as far as the dynamics is concerned. For example the potential of Vashishta *et al.* [11] produces a VDOS in poor agreement with experiment. In fact the problem with semi-empirical potentials is that the different parts are tightly bound together and further improvements are not

easily forecasted. Recently Wilson and Madden [49] have made several attempts to include a realistic description of polarization effects in ionic models using full formal charges (e.g. Si^{4+}, O^{2-}). In the case of silica [50] the inclusion of polarization effects with formal ionic charges permits the reproduction of the structure and the Si-O-Si bond angle distribution as accurately as a rigid ionic model using screened charges (e.g. TTAM) where the polarization effects are accounted for in an effective way. Moreover, the infrared spectrum [51] of silica glass is better reproduced in the low frequency region where the TTAM model fails. By the same token, Anderson *et al.* [12] have also obtained a good reproduction of the infrared spectrum in using a hybrid scheme where the anion polarizability is included explicitly in addition to screened charges on Si and O atoms (instead of formal charges as Wilson and Madden did). However the price to pay is a greater complexity to implement these kinds of potential in a MD code and a higher computer cost. Finally, in a more fundamental way it should be worthwhile to know what level of agreement with experimental data an "ab initio" molecular dynamics calculation (based upon Car-Parrinello method) could yield for the density of states and other vibrational spectra of silica (for a recent structural study with this method see [52]).

Acknowledgements

We thank the Institut du Développement et des Ressources en Informatique Scientifique (IDRIS, CNRS) for allocation of computer time on the CRAY C-98.

References

[1] Malinovky, V. K. and Sokolov, A. P. (1986). "The nature of boson peak in Raman scattering in glasses", *Solid State Commun.*, **57**, 757.

[2] Strom, U. and Taylor, P. C. (1977). "Temperature and frequency dependences of the far-infrared and microwave optical absorption in amorphous materials", *Phys. Rev. B*, **16**, 5512.

[3] Galeener, F. L., Leadbetter, A. J. and Stringfellow, M. W. (1983). "Comparison of the neutron, Raman, and infrared vibrational spectra of vitreous SiO_2, GeO_2, and BeF_2", *Phys. Rev. B*, **27**, 1052.

[4] Bermejo, F. J., Criado, A. and Martinez, J. L. (1994). "On the microscopic origin of the "boson" peak in glassy materials", *Phys. Lett. A*, **195**, 236; Levelut, C., Gaimes, N., Terki, F., Cohen-Solal, G., Pelous, J. and Vacher, R. (1995). "Glass-transition temperature: Relation between low-frequency dynamics and medium-range order", *Phys. Rev. B*, **51**, 8606.

[5] Shuker, R. and Gammon, R. W. (1970). "Raman-scattering selection-rule breaking and the density of states in amorphous materials", *Phys. Rev. Lett.*, **25**, 222.

[6] Galeener, F. L. and Sen, P. N. (1978). "Theory for the first-order vibrational spectra of disordered solids", *Phys. Rev. B*, **17**, 1928.

[7] Brawer, S. (1983). "*Ab initio* calculation of the vibrational spectra of BeF_2 glass simulated by molecular dynamics", *J. Chem. Phys.*, **79**, 4539.
[8] Boulard, B., Kieffer, J., Phifer, C. C. and Angell, C. A. (1992). "Vibrational spectra in fluoride crystals and glasses at normal and high pressures by computer simulation", *J. Non-Cryst. Solids*, **140**, 350.
[9] Garofalini, S. H. (1982). "Molecular dynamics simulation of the frequency spectrum of amorphous silica", *J. Chem. Phys.*, **76**, 3189.
[10] Della Valle, R. G. and Venuti, E. (1994). "A molecular dynamics study of the vibrational properties of silica glass", *Chem. Phys.*, **179**, 411.
[11] Jin, W., Vashishta, P. and Kalia, R. K. (1993). "Dynamic structure factor and vibrational properties of SiO_2 glass", *Phys. Rev. B*, **48**, 9359.
[12] Anderson, D. C., Kieffer, J. and Klarsfeld, S. (1993). "Molecular dynamics simulations of the infrared dielectric response of silica structures", *J. Chem. Phys.*, **98**, 8978.
[13] Tsuneyuki, S., Tsukada, M., Aoki, H. and Matsui, Y. (1988). "First-principles interatomic potential of silica applied to molecular dynamics", *Phys. Rev. Lett.*, **61**, 869.
[14] Shao, J. and Angell, C. A. (1995). "Vibrational anharmonicity and the glass transition in strong and fragile vitreous polymorphs", *Proc. XVIIth Int. Cong. Glass*, **1**, 311.
[15] van Beest, B. W. H., Kramer, G. J. and van Santen, R. A. (1990). "Force fields for silicas and aluminophosphates based on *ab initio* calculations", *Phys. Rev. Lett.*, **64**, 1955.
[16] Rustad, J. R., Yuen, D. A. and Spera, J. (1990). "Molecular dynamics of liquid SiO_2 under high pressure", *Phys. Rev. A*, **42**, 2081.
[17] Della Valle, R. G. and Andersen, H. C. (1992). "Molecular dynamics simulation of silica liquid and glass", *J. Chem. Phys.*, **97**, 2682.
[18] Guissani, Y. and Guillot, B. (1995). "A numerical investigation of the liquid-vapor coexistence curve of silica", *J. Chem. Phys.*, **104**, 7633.
[19] Horbach, J., Kob, W., Binder, K. and Angell, C. A. (1996). "Finite size effects in computer simulations of the dynamics of strong glass formers", *Phys. Rev. E*, **54**, 5897.
[20] Vollmayr, K., Kob, W. and Binder, K. (1996). "Cooling rate effects in amorphous silica: a computer simulation study", *J. Chem. Phys.*, **105**, 4714.
[21] Angell, C. A. (1995). "Formation of glasses from liquids and biopolymers", *Science*, **267**, 1924.
[22] Malinovsky, V. K., Novikov, V. N., Parshin, P. P., Sokolov, A. P. and Zemlyanov, M. G. (1990). "Universal form of the low-energy (2 to 10 meV) vibrational spectrum of glasses", *Europhys. Lett.*, **11**, 43.
[23] Dianoux, A. J. (1989). "Neutron scattering by low-energy excitations of disordered materials", *Phil. Mag. B*, **59**, 17.
[24] Carpenter, J. M. and Price, D. L. (1985). "Correlated motions in glasses studied by coherent inelastic neutron scattering", *Phys. Rev. Lett.*, **54**, 441.
[25] Buchenau, U., Prager, M., Nücker, N., Dianoux, A. J., Ahmad, N. and Phillips, W. A. (1986). "Low-frequency modes in vitreous silica", *Phys. Rev. B*, **34**, 5665.
[26] Sokolov, A. P., Rössler, E., Kisliuk, A. and Quitmann, D. (1993). "Dynamics of strong and fragile glass formers: differences and correlation with low-temperature properties", *Phys. Rev. Lett.*, **71**, 2062.
[27] Galeener, F. L. and Lucovsky, G. (1976). "Longitudinal optical vibrations in glasses: GeO_2 and SiO_2", *Phys. Rev. Lett.*, **37**, 1474.
[28] Granéli, B. and Dahlborg, U. (1989). "The vibrational motions in vitreous silica at high temperatures", *J. Non-Cryst. Solids*, **109**, 295.
[29] Jin, W., Kalia, R. K., Vashista, P. and Rino, J. P. (1993). "Structural transformation, intermediate-range order, and dynamical behavior of SiO_2 glass at high pressures", *Phys. Rev. Lett.*, **71**, 3146.
[30] Lasaga, A. C. and Gibbs, G. V. (1988). "Quantum mechanical potential surfaces and calculations on minerals and molecular clusters. I. STO-3G and 6-31G* results", *Phys. Chem. Minerals*, **16**, 29.
[31] Borysow, J., Moraldi, M. and Frommhold, L. (1985). "The collision induced spectroscopies concerning the desymmetrization of classical line shape", *Mol. Phys.*, **56**, 913.
[32] a) Velde, B. and Couty, R. (1987). "High-pressure infrared spectra of some silicate glasses", *Chem. Geol.*, **62**, 35.

b) Velde, B. and Couty, R. (1987). "High-pressure infrared spectra of silica glass and quartz", *J. Non-Cryst. Solids*, **94**, 238.
[33] Wong, P. T. T. and Whalley, E. (1970). "Infra-red and Raman spectra of glasses" *Discussions Faraday Soc.*, **50**, 94.
[34] Stolen, R. H., Krause, J. T. and Kurkjian, C. R. (1970). "Raman scattering and far infrared absorption in neutron compacted silica", *Disussions Faraday Soc.*, **50**, 103.
[35] Neuroth, Von N. (1956). "Über die bestimmung der optischen konstanten n, χ aus reflexionsmessungen", *Z. Physik*, **144**, 85.
[36] Markin, E. P. and Sobolev, N. N. (1960). "Infrared reflection spectrum of boric anhydride and fused quartz at high temperatures", *Optics and Spectroscopy*, **9**, 309.
[37] Gaskell, P. H. (1966). "Thermal Properties of silica: Part I. Effect of temperature on infrared reflection spectra of quartz, cirstobalite and vitreous silica", *Trans. Faraday Soc.*, **62**, 1493.
[38] a) Williams, Q. and Jeanloz, R. (1988). "Spectroscopic evidence for pressure-induced coordination changes in silicate glassses and melts", *Science*, **239**, 902.
b) Williams, Q., Hemley, R. J., Kruger, M. B. and Jeanloz, R. (1993). "High-Pressure infrared spectra of α-quartz, coesite, stishovite and silica glass', *J. Geophys. Res.*, **98**, 22, 157.
[39] a) Madden, P. A., O' Sullivan, K., Board, J. A. and Fowler, P. W. (1991). "Light scattering by alkali halide melts: A computer simulation study", *J. Chem. Phys.*, **94**, 918.
b) Madden, P. A. and O' Sullivan, K. (1991). "The Raman spectra of alkali halide melts: a theoretical description", *J. Chem. Phys.*, **95**, 1980.
[40] Tabisz, G. C. and Neuman, M. N. "Collision-and interaction-induced spectroscopy", Kluwer Academic Publishers (Dordrecht, 1995), NATO ASI series, series C, vol. 452.
[41] Fowler, P.W. and Madden, P. A. (1985). "Fluctuating dipoles and polarizabilities in ionic materials: calculations of LiF", *Phys. Rev. B*, **31**, 5443.
[42] Gaskell, P. H. and Wallis, D. J. (1996). "Medium-range order in silica, the canonical network glass", *Phys. Rev. Lett.*, **76**, 66.
[43] McMillan, P., Piriou, B. and Couty, R. (1984). A Raman study of pressure-densified vitreous silica", *J. Chem. Phys.*, **81**, 4234; Hemley, R. J., Mao, H. K., Bell, P. M. and Mysen, B. O. (1986). "Raman spectroscopy of SiO_2 glass at high pressure", *Phys. Rev. Lett.*, **57**, 747.
[44] McMillan, P., Poe, B. T. Gillet, Ph. and Reynard, B. (1994). "A study of SiO_2 glass and supercooled liquid to 1950 K via high-temperature Raman spectroscopy", *Geochim. Cosmochim. Acta*, **58**, 3653.
[45] Barrat, J. L., Badro, J. and Gillet, P. (1996). "Strong to fragile transition in a model of liquid silica", *Mol. Sim.*, this volume.
[46] Della Valle, R. G. and Andersen, H. C. (1991). "Test of a pairwise additive ionic potential model for silica", *J. Chem. Phys.*, **94**, 5056.
[47] Cowley, E. R. and Gross, J. (1991). "Lattice dynamics of a pair-potential model of α-quartz", *J. Chem. Phys.*, **95**, 8357.
[48] Tse, J. S. and Klug, D. D. (1991). "The structure and dynamics of silica polymorphs using a two-body effective potential model", *J. Chem. Phys.*, **95**, 9176; Badro, J., Barrat, J. L. Gillet, Ph. (1996). "Numerical simulation of α-quartz under nonhydrostatic compression: memory glass and five-coordinated crystalline phases", *Phys. Rev. Lett.*, **76**, 772.
[49] Wilson, M. and Madden, P. A. (1993). "Polarization effects in ionic systems from first principles" *J. Phys.: Condens. Matter*, **5**, 2687; Wilson, M. and Madden, P. A. (1993). "Short-and intermediate-range order in MCl_2 melts: the importance of anionic polarization", *J. Phys.: Condens. Matter*, **5**, 6833.
[50] Wilson, M. and Madden, P. A. (1994). "Polarization effects on the structure and dynamics of ionic melts", *J. Phys.: Condens. Matter*, **6**, A 151.
[51] Wilson, M., Madden, P. A., Hemmati, M. and Angell, C. A. (1996). "Polarization effects, network dynamics, and the infrared spectrum of amorphous SiO_2", *Phys. Rev. Lett.*, **77**, 4023.
[52] Sarnthein, J., Pasquarello, A. and Car, R. (1995). "Structural and electronic properties of liquid and amorphous SiO_2: An *ab initio* molecular dynamics study", *Phys. Rev. Lett.*, **74**, 4682.